Magnetic Behavior of Single $La_{0.67}Ca_{0.33}MnO_3$ Nanotubes: Surface and Shape Effects

M. I. Dolz, W. Bast, D. Antonio, H. Pastoriza, J. Curiale, and R. D. Sánchez

Centro Atómico Bariloche, Comisión Nacional de Energía Atómica,

Av. Bustillo 9500, R8402AGP S. C. de Bariloche, Argentina

A. G. Leyva

Centro Atómico Constituyentes, Comisión Nacional de Energía Atómica,

Av. Gral Paz 1499 (1650) San Martín, Argentina

(Dated: March 14, 2008)

Abstract

We report magnetization experiments in two magnetically isolated ferromagnetic nanotubes of perovskite $La_{0.67}Ca_{0.33}MnO_3$. The results show that the magnetic anisotropy is determined by the sample shape although the coercive field is reduced by incoherent magnetization reversal modes. The temperature dependence of the magnetization reveals that the magnetic behavior is dominated by grain surface properties. These measurements were acquired using a Silicon micro-mechanical oscillator working in its resonant mode. The sensitivity was enough to measure the magnetic properties of these two samples with a mass lower than 14 picograms and to obtain for the first time the magnetization loop for one isolated nanotube.

PACS numbers: 75.75.+a,85.85.+j,75.47.Lx

Keywords: manganite, nanotube, MEMS

I. INTRODUCTION

Manganites are complex oxides that adopt a pseudo-cubic perovskite crystal structure. The discovery of colossal magnetoresistance in films of these materials [1] was a great leap for the field of spintronics. The first impact was its use as electrodes in magnetic tunnel junctions [2], giving tunnel magnetoresistance ratios one order of magnitude larger than of those obtained with transition-metal electrodes. The fabrication of manganite nanotubes are nowadays on the rise due to their several possible technological applications. These nanotubes could impact on technology in different ways. One possible application is in solid-oxide fuel cells. Manganites nanotubes make good cathodes thanks to their granular structure where gases may be efficiently distributed and because they conduct both electrons and oxygen ions, and are resistant to high-temperature oxidizing environments [3]. Another very important possible application of metallic manganites nanotubes in the field of nanotechnology is as highly localized sources of electrons possessing spins of a particular orientation, which can be perfectly aligned [4]. Manganite also exhibit challenging electronic and magnetic properties because of their tendency to present coexistence of different phases in a wide range of scale lengths [5]. The relative quantity of phases coexisting can be modified by means of small external forces due to the strong competition between the present interactions. The ability to fabricate nanotubes (NT) of these compounds has recently been demonstrated [6]. These nanostructures are usually studied by measurements in large sets where the intrinsic response of individual structures is clouded by the global response. Given the necessity of having a good characterization and knowledge of each of these complex nanostructures this work is oriented towards the study of individual $La_{0.67}Ca_{0.33}MnO_3$ (LCMO) NT magnetic properties.

In this paper, we show that the saturation magnetization temperature dependence obtained for two isolated NT is clearly different from the bulk sample. We observe a lineal temperature dependence. This behavior is explained having in mind the predominating surface effects of each grain that constitutes a NT [7, 8, 9]. This granular structure favors the existence of weak collective modes for the magnetization reversal that depress NT coercive fields (H_c) respect to that expected by the shape anisotropy constant. But, the complete magnetization loop obtained for one single NT shows a little increment of H_c respect to those measured in a powder of NT and in a bulk sample [10]. One of the main achievements

of our work has been to obtain for the first time the complete loop of magnetization of one isolated NT.

On the subject of measuring magnetic properties of small samples, several approaches have been reported in the literature: microSQUIDs [11], which are very sensitive but constrained to low fields and low temperatures; Alternate Gradient Magnetometers (AGM) [12] have also demonstrated high sensitivity [13] but quantitative measurements are difficult to obtain since the measured signal strongly depends on the sample shape and on the exact location of the sample in the field gradient [14]. Central to our approach is the use of Micromechanical torsional oscillators as magnetometers. These systems fabricated with MEMS technology, extend all the advantages of high-Q mechanical oscillators measurements [15] to the microscopic scale and, before focusing on the results of this paper, we will explain how it is possible to measure magnetic properties with these MEMS.

II. EXPERIMENTAL

In our experiments we used a variant of the micro-torsional oscillators presented by Bolle *et al.* [16]. These poly-silicon oscillators were fabricated in the MEMSCAP [17] foundry using its Multiuser process (MUMPS). Each oscillator consists of a 44×106 μm^2 released plate anchored to the substrate by two serpentine springs. Fixed to the substrate, underneath the plate, two electrodes are used for the driving and motion detection. A 100 mV peak-to-peak ac voltage is applied between one electrode and the plate to induce the motion, and the change in capacitance is detected in the other electrode using a Phase Sensitive Detection scheme tuned at twice the driving frequency. A more detailed description of the experimental detection setup can be found elsewhere [18].

A powder of NT of LCMO was fabricated by the pore-filling method [19]. With this procedure NT are build from grains of 25 nm in diameter [10]. A small amount of the obtained conglomerated NT was placed on a lithographically patterned substrate where individual NT were identified and selected using a scanning electron microscope (SEM). The chosen NT were placed on top of a silicon micro-oscillator [18] using hydraulic micromanipulators under an optical microscope, and were glued to it with a sub-micrometer drop of Apiezon© N grease. In Fig. 1(b) we show a scanning electron micrograph of the two NT glued on top of the MEMS oscillator. All the results reported in this paper

correspond to measurements done in two NT of 700 nm in diameter and 9.5 μm in length placed perpendicular to the rotation axis of the oscillator and separated 40 μm (See Fig. 1(b)). At this distance the interaction between the NT is negligible as the dipolar magnetic field, estimated from the expected maximum magnetization value, is slightly larger than the earth magnetic field and two orders of magnitude lower than the necessary field to reverse the magnetization of the NT. The measurements were taken in vacuum inside a closed-cycle cryogenerator where the temperature can be varied between 14 and 300 K. The magnetic field was provided by a split electromagnet that can be rotated in the plane perpendicular to the axis of rotation of the oscillators with an accuracy of 1 °.

The experiment consists in measuring the oscillator's torsional mode resonant frequency as a function of magnetic field and temperature. This is accomplished by sweeping the driving frequency and detecting the oscillator amplitude. The measured amplitude is squared and fitted with a lorentzian function, from which the resonant frequency and quality factor are obtained. The natural resonant frequency (ν_0) of an oscillator in the torsional mode is given by: $2\pi\nu_0 = \sqrt{\frac{k_e}{I}}$, where $k_e \simeq 7.82 \times 10^{-3}\,\mathrm{dyn \cdot cm}$ is the elastic restorative constant of the serpentine springs and $I = 3.8 \times 10^{-14}\,\mathrm{g \cdot cm^2}$ is the plate's moment of inertia. In our oscillators this mode has a resonant frequency close to 72200 Hz and a quality factor Q greater than 5×10^4, which means that the width of the resonant peak is less than 2 Hz.

When we attach a magnetic sample to the oscillator the resonant frequency ν_r changes to:

$$2\pi\nu_r = \sqrt{\frac{k_e + k_M}{I}}, \tag{1}$$

where k_M is the variation in the effective elastic constant originated by the magnetic interaction between the sample and the external magnetic field. For the experimental conditions I does not change during the measurements and $\Delta\nu << \nu_0$. Therefore it is possible to express

$$k_M \simeq 8\pi^2 I \nu_0 \Delta\nu, \tag{2}$$

where $\Delta\nu$ is the change in the resonant frequency. This change as a function of a magnetic field applied parallel to the principal axis of the NT at different temperatures is showed in Fig. 2(a). These results show that the oscillator is sensitive enough to detect the NT magnetic response.

In our experiment the oscillatory motion produces a tilt between the fixed magnetic field and the NT axis. At high magnetic fields, when the magnetization of the sample is saturated,

$M = M_s$ and $\frac{dM}{dH} = 0$, the change in the resonant frequency can be written as [20]:

$$\frac{1}{8\pi^2 I \nu_0 \Delta\nu} \simeq \frac{1}{k_M} = \frac{1}{2KV} + \frac{1}{M_S V H_0} \tag{3}$$

where $\Delta\nu$ is the change in the resonant frequency at a given magnetic field, V is the sample volume, and $K = \frac{1}{2} N M_S^2$ is the shape anisotropy energy density. From a linear square fit of the high magnetic fields data the values for $M_S V$ and K are obtained. In Fig. 2(b) we plot $\Delta\nu^{-1}$ vs H_0^{-1} for the data taken at some selected temperatures showing the excellent correlation obtained with this linear fit in a wide range of fields. K depends on temperature and its extrapolated value at $T = 0$K is 1.24×10^{-6} erg.

III. RESULTS AND DISCUSSION

The saturation magnetization temperature dependence of our NT obtained with the described procedure is plotted in Fig. 3. For comparison we have plotted in the same graph the results obtained for a 0.40 mg piece of sintered LCMO taken in a commercial SQUID magnetometer with an applied field of 10 kOe. Clearly the temperature dependence of the individual NT magnetization differs from the bulk ferromagnet.

Magnetization measurements done in samples of varying sizes [7] have shown that the diminution of grain size is associated with a decrease on the magnetization and a change in the temperature dependence. The sample size reduction implies an increase on the surface to volume ratio which means that surface effects become more relevant to describe the physical behavior of the sample. At the surface of crystalline grains the atomic coordination is reduced and atomic disorder is much more important than in the bulk. In Manganese-based perovskites the magnetic properties result from the interplay of many complex phenomena. The ferromagnetic double-exchange spin–spin coupling competes with an anti-ferromagnetic super exchange. Both are very sensitive to the Mn-O-Mn bond angle and distance. This implies that the magnetization at the surface of these compounds is highly susceptible to surface conditions. The magnetic modifications at the surface are usually argued as the origin of a magnetic dead layer, but in general it affects in a more complex way the magnetic properties. The detailed description of the surface magnetism temperature dependence is strongly dependent on the surface local conditions. In a mean field calculation it has been shown [8] that the surface magnetization has a linear temperature dependence. Photo-emission

measurements of the surface magnetization performed in other manganese perovskite compounds [9] show this linear temperature dependence, as obtained in our experiments. Taking into account that our NT are built-up from grains of 25 nm in diameter [10] and the surface magnetism could extend 2 nm in depth, approximately 50 % of the magnetic moments are weakly correlated on the surface and dominate the global magnetic behavior.

The volume for the two NT is $2.32 \times 10^{-12}\,\mathrm{cm}^3$, it was estimated from the external dimensions measured in a SEM and assuming a nominal wall thickness of 60 nm [10]. Considering this volume and the bulk manganite density $6.03\,\mathrm{g/cm}^3$ [21], their total mass is about $14 \times 10^{-12}\,\mathrm{g}$. In consequence, the saturation magnetization per mass extrapolated to 0 K is 52 emu/g (See Fig. 3) which is greater than the value obtained for a powder of these NT [10] and is less than the bulk LCMO value (98 emu/g). The difference with the bulk's value can be assumed by the existence of a *magnetic dead layer* in each grain that constitutes the wall of the NT. Considering that the ratio between the obtained saturation magnetization and the bulk value (0.53) should be equal to the ratio between the magnetic core and the total grain volume (with an average diameter of 26 nm [10]), we can estimate the width of this magnetic dead layer. Its estimated value is around 2 nm and is very close to the 1.6 ± 0.4 nm value obtained from the saturation magnetization of a powder of randomly oriented NT. Due to the granular morphology of the NT, the dead layer thickness obtained from our results must be taken as a superior limit. The NT density is smaller than the bulk, which means that the real mass of the NT is lower than calculated and the dead layer is smaller.

In order to obtain the full magnetization loop in our experiments it must be noted that the restorative constant k_M generated by the magnetic sample has to be evaluated through the second derivative of the magnetic free energy respect to the displacement angle θ between the sample and the magnetic field. The magnetic energy density for a ferromagnetic sample with uniaxial anisotropy in a magnetic field can be described by:

$$\begin{aligned} E = & \quad -\vec{\mathbf{M}} \cdot \vec{\mathbf{H}}_{\mathbf{0}} + \frac{1}{2} N |\vec{\mathbf{M}}|^{\mathbf{2}} \sin^{\mathbf{2}}(\varphi) \\ = & \quad -M H_0 \cos(\theta - \varphi) + \frac{N M^2}{2} \sin^2(\varphi) \end{aligned} \tag{4}$$

where $\vec{M}$ is the sample magnetization, $\vec{H}_0$ is the external magnetic field, N is the difference between the demagnetization factors of the magnetic hard and easy directions, and φ is the angle between the magnetization vector and the easy direction of the sample (See Fig. 1(a)).

This angle has to be calculated from the evaluation of $\frac{dE}{d\varphi}|_\theta = 0$ for a given θ. Taking into account that M depends on $H = H_0 - H_D$ (H_D the demagnetizing field) and φ depends on θ, for θ close to zero:

$$\begin{aligned} \frac{1}{V}k_M = & \quad \frac{d^2E}{d\theta^2} \\ = & \quad \frac{MNH_0\left[M(MN+H_0)+\frac{dM}{dH}H_0(MN+2H_0)\right]}{(MN+H_0)^2}. \end{aligned} \tag{5}$$

The complete magnetization loop can be obtained from the measured k_M data through a nonlinear least-squared fit. In this procedure we used M and $\chi = \frac{dM}{dH}$ as free field dependent parameters and N as a fixed parameter obtained from the fitting of the data at high fields.

In Fig. 4 we plot $m(H)$ obtained from our measurements at 14 K. In the same graph we have plotted the hysteresis loop for a 1.84 mg sample of NT powder measured in a SQUID magnetometer at the same temperature. There is an excellent agreement between both measurements. In the randomly oriented NT powder the measurement shows an S shaped curve originated from the distribution of anisotropies in the sample. In contrast the isolated NT measurement is more abrupt, as expected.

More information can be extracted from the raw $\Delta\nu$ vs H data. From equation (5) we have $\Delta\nu(H_0) = 0$ when $H_0 = 0$ or $M(H_0) = 0$, the later corresponding to the H_c. These zero-crossing points are visible in the data presented in the inset of Fig. 2(a). The values obtained for the H_c ($\approx 350\,\mathrm{Oe}$) are much smaller than those expected for a H_c produced by the shape anisotropy constant obtained from our data ($\approx 3320\,\mathrm{Oe}$), but are slightly larger than those measured in a powder of NT (as shown in Fig. 4). Considering the granular structure of our NT and a weak magnetic interaction between grains, the existence of weak collective modes for the magnetization reversal could be favored (i.e. as fanning or buckling of the magnetic moments) which would result in a depressed NT H_c.

IV. CONCLUSIONS

In conclusion, we have presented magnetization measurements of single LCMO granular NT using a silicon micro-oscillator. Thanks to the oscillator's high Q factor and soft restorative constant we have obtained a sensitivity better than 10^{-10} emu. With this sensibility we can obtain the magnetization loop for two NT of a total mass of only 14 pg. The temperature dependence and the magnetization values indicate that the ferromagnetic alignment of the

moments are affected by the grain surface, where the spin coupling is reduced from that at the core of each particle. The results are consistent with those of a ferromagnetic material with the shape anisotropy given by a cylindrical geometry. The measured H_c suggests the existence of magnetization reversal processes that can overcome the energy barrier given by this anisotropy constant.

V. ACKNOWLEDGMENTS

This work was partially supported by ANPCyT grant PICT04-03-21372. M. I. D., D. A. and J. C. fellowship holders of CONICET. R. D. S. and H. P. research members of CONICET. We thank F. de la Cruz for a careful reading of the manuscript.

---

[1] S. Jin, T. H. Tiefel, M. McCormack, R. A. Fastnacht, R. Ramesh, and L. H. Chen, Science **264**, 413 (1994).

[2] Y. Lu, W. Li, G. Gong, G. Xiao, A. Gupta, P. Lecoeur, J. Sun, Y. Wang, and V. Dravid, Phys. Rev. B **54**, R8357 (1996).

[3] A. G. Leyva, J. Curiale, H. Troiani, M. Rosenbusch, P. Levy, and R. D. Sánchez, Advances and Science and Technology **51**, 54 (2006).

[4] M. Bowen, M. Bibes, A. Barthlmy, J. P. Contour, A. Anane, and Y. Lemaitre, Appl. Phys. Lett. **82**, 233 (2003).

[5] N. Mathur and P. Littlewood, Physics Today **56**, 25 (2003).

[6] P. Levy, A. G. Leyva, H. Troiani, and R. D. Sánchez, Appl. Phys. Lett. **83**, 5247 (2003).

[7] R. D. Sánchez, J. Rivas, C. Vázquez-Vázquez, A. López-Quintela, M. T. Causa, M. Tovar, and S. Oseroff, Appl. Phys. Lett. **68**, 134 (1996).

[8] T. Kaneyoshi, *Introduction to Surface Magnetism* (CRC Press, Inc., Boca Raton, Florida, USA, 1990), ISBN 0-8493-6687-9.

[9] J.-H. Park, E. Vescovo, H.-J. Kim, C. Kwon, R. Ramesh, and T. Venkatesan, Phys. Rev. Lett **81**, 1953 (1998).

[10] J. Curiale, R. D. Sánchez, H. E. Troiani, C. Ramos, H. Pastoriza, A. G. Leyva, and P. Levy, Phys. Rev. B **75**, 224410 (2007).

[11] W. Wernsdorfet, B. Doudin, D. Mailly, K. Hasselbach, A. Benoit, J. Meier, J.-P. Ansermet, and F. Barbara, Phys. Rev. Lett. **77**, 1873 (1996).

[12] H. Zijlstra, Rev. Sci. Instrum. **41**, 1241 (1970).

[13] M. Todorovic and S. Schultz, Appl. Phys. Lett. **73**, 3595 (1998).

[14] M. Barbic, Rev. Sci. Instrum. **75**, 5016 (2004).

[15] R. N. Kleiman, G. K. Kaminsky, J. D. Reppy, R. Pindak, and D. J. Bishop, Rev. Sci. Intrum. **56**, 2088 (1985).

[16] C. A. Bolle, V. Aksyuk, F. Pardo, P. L. Gammel, E. Zeldov, E. Bucher, R. Boie, D. J. Bishop, and D. R. Nelson, Nature **399**, 43 (1999).

[17] MEMSCAP Inc., 4021 Stirrup Creek Drive, Durham, NC 27703, USA, URL `http://www.memscap.com`.

[18] M. Dolz, D. Antonio, and H. Pastoriza, Physica B **398**, 329 (2007).

[19] A. G. Leyva, P. Stoliar, M. Rosenbusch, V. Lorenzo, P. Levy, C. Albonetti, M. Cavallini, F. Biscarini, H. E. Troiani, J. Curiale, et al., J. Solid State Chem. **177**, 3949 (2004).

[20] J. Morillo, Q. Su, B. Panchapakesan, M. Wuttig, and D. Novotny, Rev. Sci. Instrum. **69**, 3908 (1998).

[21] M. C. Sanchez, J. Blasco, J. Garca, J. Stankiewicz, J. M. D. Teresa, and M. R. Ibarra, J. Solid State Chem. **138**, 226 (1998).

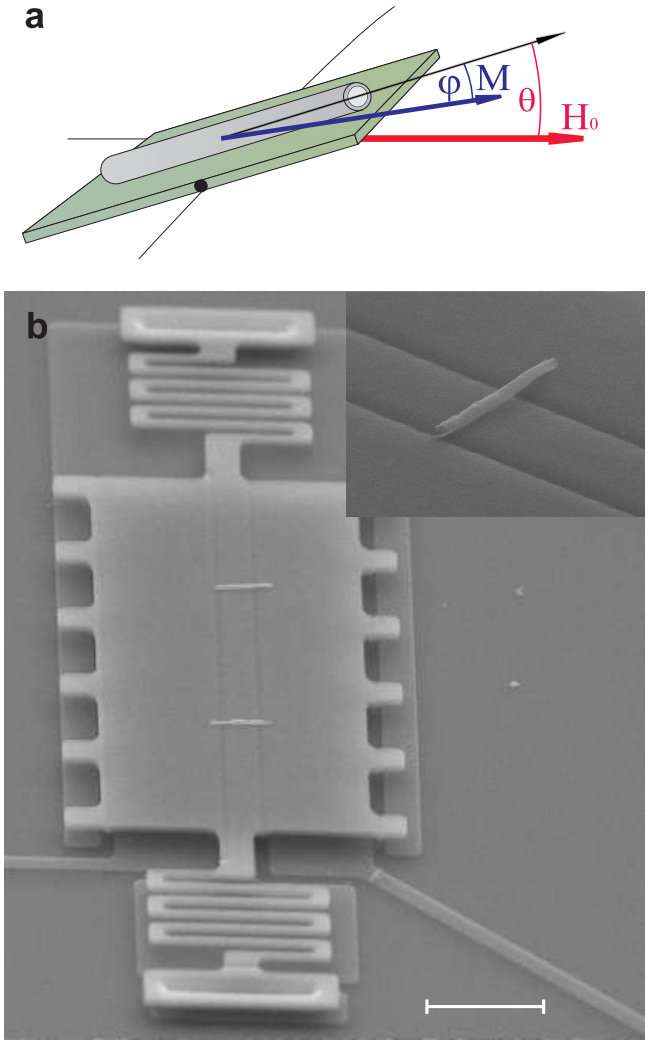

FIG. 1: (a) Sketch of the different angles used in the analysis of the measurements. (b) Scanning electron microscope image of the LCMO nanotubes mounted on top of the polysilicon micro-oscillator. The image was taken at an angle of 50 degrees to enhance the topographic contrast. The dimension scale bar corresponds to 20 μm. The inset shows a zoom in one of the nanotubes.

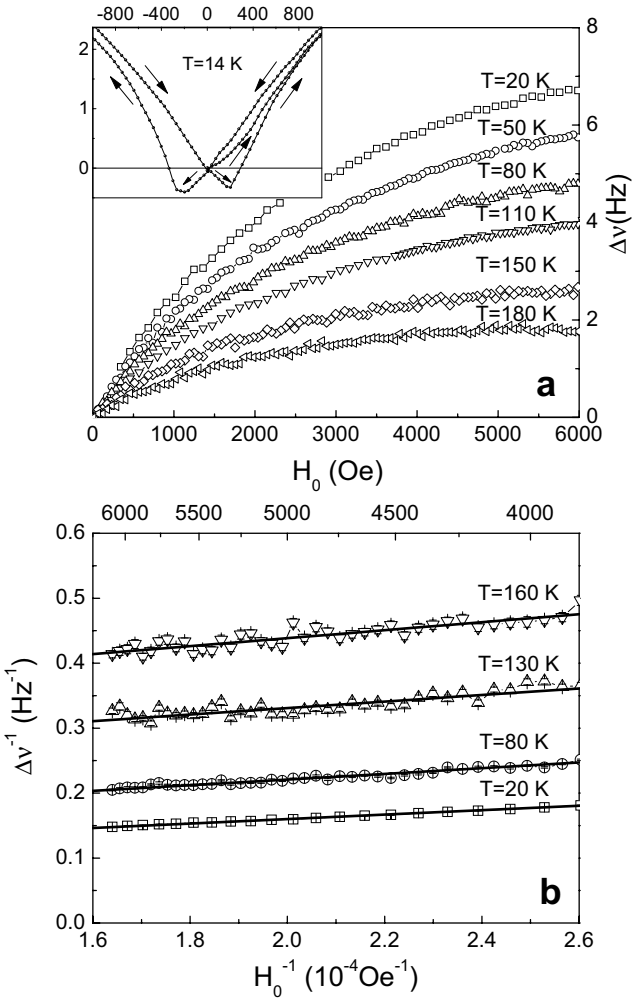

FIG. 2: (a) Change in the resonant frequency as a function of the external magnetic field for different temperatures as indicated in the figure. The inset shows a zoomed area close to zero magnetic field for a temperature of 14 K. The arrows indicate the direction of the magnetic field sweep in each branch of the measurement. (b) Inverse of the frequency change as a function of the inverse of the applied magnetic field for high H_0 values is plotted for some selected temperatures (indicated in the graph). The solid lines are fits of the data, which allows to obtain the saturation magnetization and the shape anisotropy constant.

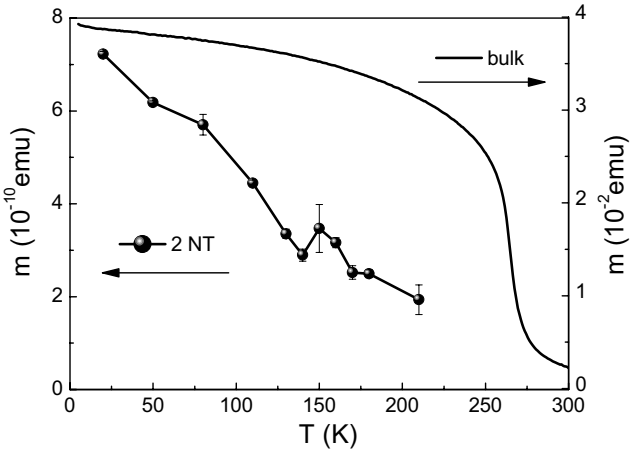

FIG. 3: Saturation magnetization as a function of temperature. Bullets are the data obtained from the measurements on two isolated LCMO nanotubes. Solid line represents the magnetization of LCMO bulk sample for an applied magnetic field of 10 kOe.

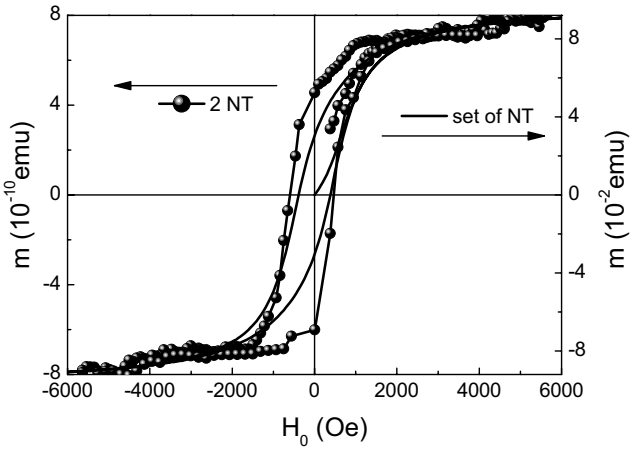

FIG. 4: Comparison between the hysteresis loop of two isolated LCMO nanotubes obtained with the torsional micro-oscillator magnetometer (bullets) and the loop data of 1.84 mg of randomly oriented nanotubes taken with a commercial SQUID magnetometer (continuous line).